

## P4.19 Multilayered Clouds Identification and Retrieval for CERES Using MODIS

Sunny Sun-Mack<sup>1</sup>, Patrick Minnis<sup>2</sup>, Yan Chen<sup>1</sup>, Yuhong Yi<sup>3</sup>, Jainping Huang<sup>3</sup>, Bin Lin<sup>2</sup>, Alice Fan<sup>1</sup>, Sharon Gibson<sup>1</sup>,  
and Fu-Lung Chang<sup>4</sup>

<sup>1</sup>Science Application International Corporation, Hampton, VA 23666

<sup>2</sup>Climate Science Branch, NASA Langley Research Center, Hampton, VA 23681

<sup>3</sup>AS & M, Hampton, VA 23666

<sup>4</sup>National Institute of Aerospace, Hampton, VA 23666

### 1. INTRODUCTION

Traditionally, analyses of satellite data have been limited to interpreting the radiances in terms of single-layer clouds. Generally, this results in significant errors in the retrieved properties for multilayered cloud systems. Two techniques for detecting overlapped clouds and retrieving the cloud properties using satellite data are explored to help address the need for better quantification of cloud vertical structure. The first technique was developed using multispectral imager data with secondary imager products (infrared brightness temperature differences, BTD). The other method uses microwave (MWR) data. The use of BTD, the 11-12  $\mu\text{m}$  brightness temperature difference, in conjunction with  $\tau$ , the retrieved visible optical depth, was suggested by Kawamoto et al. (2001) and used by Pavlonis et al. (2004) as a means to detect multilayered clouds. Combining visible (VIS; 0.65  $\mu\text{m}$ ) and infrared (IR) retrievals of cloud properties with microwave (MW) retrievals of cloud water temperature  $T_w$  and liquid water path  $LWP$  retrieved from satellite microwave imagers appears to be a fruitful approach for detecting and retrieving overlapped clouds (Lin et al., 1998, Ho et al., 2003, Huang et al., 2005). The BTD method is limited to optically thin cirrus over low clouds, while the MWR method is limited to ocean areas only. With the availability of VIS and IR data from the Moderate Resolution Imaging Spectroradiometer (MODIS) and MW data from the Advanced Microwave Scanning Radiometer EOS (AMSR-E), both on *Aqua*, it is now possible to examine both approaches simultaneously. This paper explores the use of the BTD method as applied to MODIS and AMSR-E data taken from the *Aqua* satellite over non-polar ocean surfaces.

### 2. DATA

Data from the MODIS and AMSR-E on the *Aqua* satellite are used to perform the various retrievals. The 1-km MODIS data are analyzed for CERES using the VIS-IR-Solar-infrared-Split-window Technique (VISST; Minnis et al., 1995) to retrieve single-layer (SL) cloud

properties for each pixel. The CERES cloud retrieval output, which includes cloud properties such as  $\tau$  and cloud effective temperature  $T_c$ , as well as the original pixel radiances at 0.64, 1.6, 2.1, 3.7, 11, and 12, 1.3, 4.0, 6.7, 8.5, 13.3, 13.5, 13.9, and 14.2- $\mu\text{m}$  MODIS channels. Cloud  $LWP$  and  $T_w$  are derived from the AMSR-E MW data at the 12-km resolution, 36.5-GHz field of view (FOV) by matching the multispectral MW data to radiative transfer model (RTM) calculations (Lin et al., 1998). The CERES pixel-level results are then convolved into the AMSR-E footprints following an earlier approach (Ho et al., 2003) in order to apply the MW-VIS-IR multilayered cloud detection method of Huang et al. (2005). In this pilot study, the CERES MODIS pixels are matched to the nominal nadir-size footprint of the AMSR-E to facilitate comparison of the different techniques.

The comparative analyses focus on 18 5-minute *Aqua* MODIS granules taken over 8 days from January 2 - 9, 2005. The RGB MODIS image in Figure 1 shows a complex system with a mixture of ice (pinkish, grayish), liquid water (white, yellow, and peach), and overlapped clouds. Also shown are the VISST-retrieved values of  $\tau$  for all cloud types assuming SL clouds. The cloud optical depths range from 0.3 up to 128.

### 3. METHODOLOGIES

Two different ML cloud techniques are compared here; the MW-VIS-IR Multilayer Cloud Detection System (MCRS; Huang et al., 2005) and the CERES-BTD method (Minnis et al., 2005). The MCRS is used as the reference technique because it can detect water clouds over ocean in the presence of ice clouds as long as no precipitation occurs.

#### 3.1 MCRS

The MW-VIS-IR is used only if the VISST retrieves at least 98% ice cloud coverage for the MODIS pixels in the convolved AMSR field of view and the solar zenith angle is less than 78°. The scene is classified as being composed of SL ice clouds, if the retrieved MW  $LWP \leq 40 \text{ gm}^{-2}$ . If  $LWP > 40 \text{ gm}^{-2}$ ,  $T_w - T_c > 5 \text{ K}$ , and no precipitation is detected, the scene is classified as ML ice clouds, that is, an ice over a water cloud system. The precipitation detection is based on the amount of

\*Corresponding author address: Sunny Sun-Mack, SAIC, 1 Enterprise Pkwy., Hampton, VA, 23666. email: s.sun-mack@larc.nasa.gov.

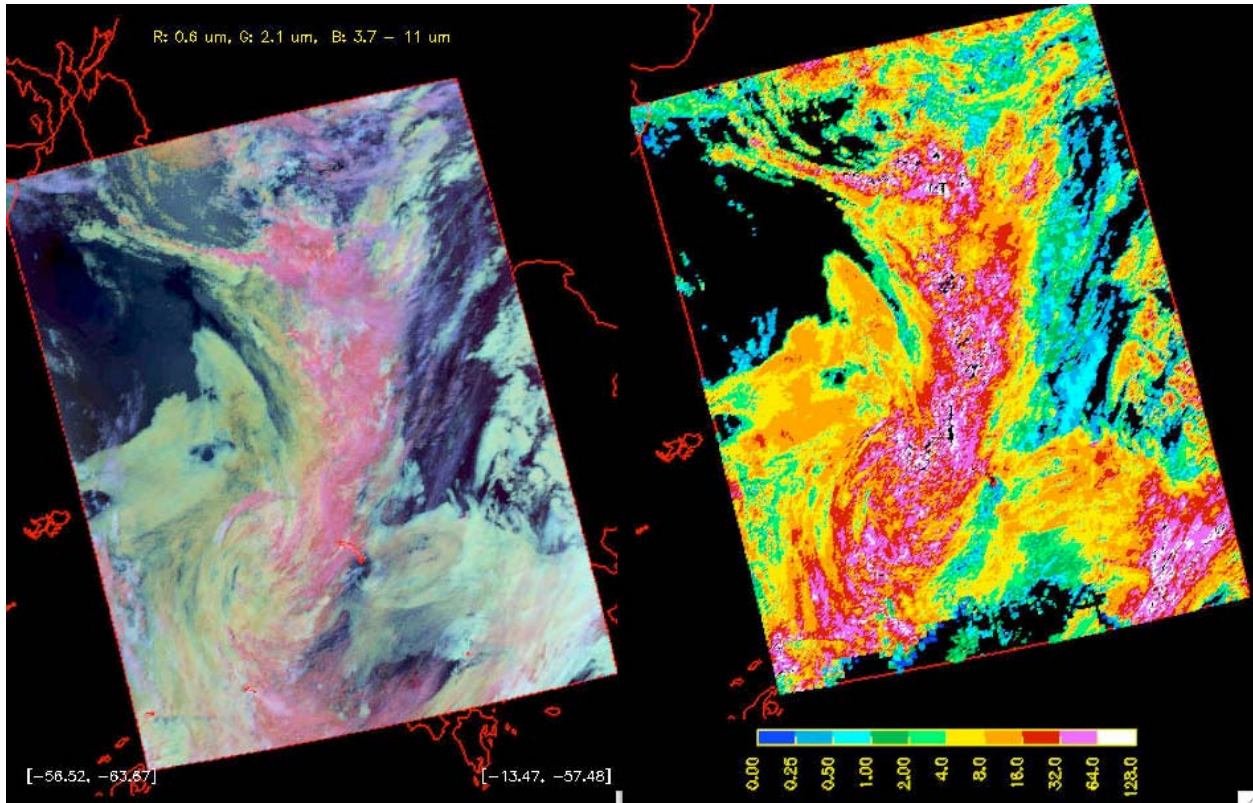


Fig. 1. CERES imagery for multilayer cloud detection comparisons for 1645 UTC, January 5, 2005. Left: *Aqua* MODIS pseudo-color RGB image. Right: VISST-derived cloud optical depths.

polarization in the 36.5-GHz channel. Single-layer water, clear, partly cloudy, and mixed phase scenes are not considered here. Figure 2 shows the probability of ice over water by MW-VIS-IR method. Multilayer probability is considered to be the highest (red) when  $T_w - T_c \geq 15$  K. The eighteen *Aqua* MODIS granules chosen in this study are from these highly likely multilayer clouds regions.

### 3.2 CERES-BTD

The CERES-BTD is a technique, following the suggestion of earlier research (e.g., Kawamoto et al., 2001) that uses the VISST-derived parameters and the BTD to classify cloudy pixels as SL, ML, or indeterminate. Figure 3 shows the flow diagram for the CERES-BTD. It begins with the VISST retrieval and applies different tests depending on the phase of the SL retrieval. In addition to  $\tau$ , the CERES-BTD uses either the effective ice crystal diameter  $D_e$  or  $r_e$  depending on the phase. No iteration is performed in this prototype version.

An additional set of tests is applied if the cloud is ice and  $\tau(\text{VISST}) > 20$ . Sometimes, a thick high ice cloud can have a positive BTD if the cloud top is diffuse. The cloud layering is classified as indeterminate if any one of the following statements is true.

- $-0.5 \text{ K} < \text{BTD} < 0.5 \text{ K}$ .
- $3.0 \text{ K} < T - T(3.7 \mu\text{m}) < 3.0 \text{ K}$ .
- $-3.0 \text{ K} < T - T(4.0 \mu\text{m}) < 3.0 \text{ K}$ .
- $-3.0 \text{ K} < T - T(6.7 \mu\text{m}) < 3.0 \text{ K}$ .
- $-0.5 \text{ K} < T - T(8.5 \mu\text{m}) < 0.5 \text{ K}$ .
- $-3.0 \text{ K} < T - T(13.3 \mu\text{m}) < 3.0 \text{ K}$ .

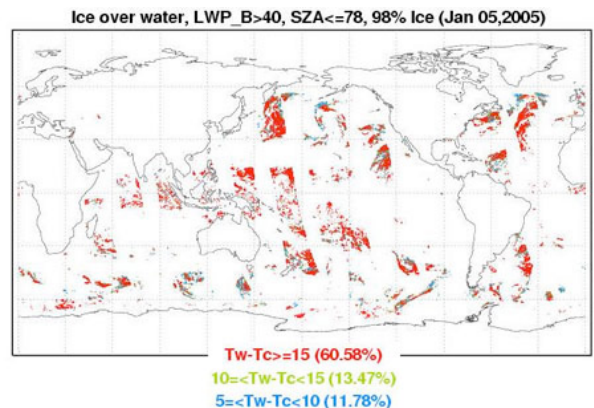


Fig. 2. Multilayer clouds probability obtained from MW-VIS-IR with the highest probability - red, the lowest - blue, and the middle - green.

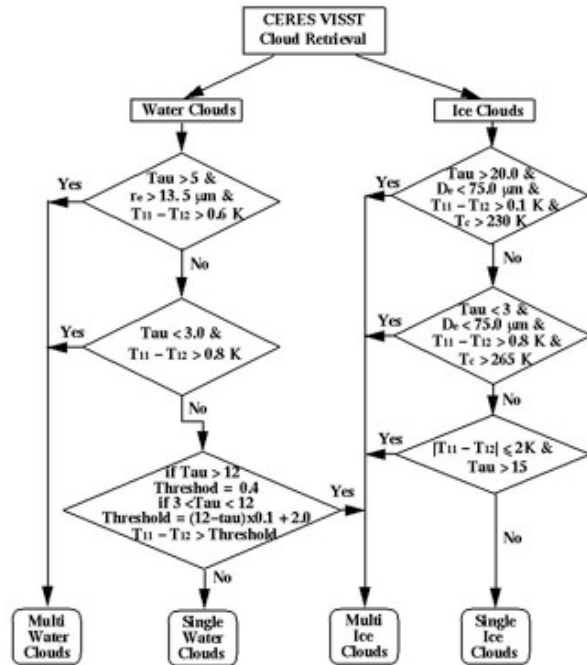


Fig. 3. Flow chart for classifying VISST retrievals as single or multi-layered clouds in the CERES-BTD Method.

An example of the CERES-BTD applied to *Aqua* MODIS data is shown in Fig. 4 for a match with the Cloud Physics Lidar (McGill et al., 2004) (CPL) on the ER-2 as it flew over the Gulf of Mexico during 26 July 2002. The CPL detects a thin cirrus layer (Figure 4a) between 13 and 15 km above scattered cumulus clouds between 0.5 and 2 km. The BTD (Fig. 4b) along the flight path varies between 2 and 4 K with larger values coinciding with slightly thicker cirrus and the absence of cumulus clouds. The CERES-BTD classification (Figure 4c) detects ML clouds only when the lower cloud appears to be thick (bright) in the CPL return. Although some ML clouds are misclassified as SL, most of the SL clouds are accurately designated. The retrieval method yields mixed results for cloud heights (Figure 4d). At 18.3 UTC, it produces only a slight separation between the high (red) and low (blue) clouds, possibly because the low cloud height was incorrectly specified as being too high. At 18.37 UTC, the clouds are correctly classified as SL and the VISST (black) places the cloud between 9 and 10 km. The effective cloud height from VISST should be located somewhere between the cloud base and top. The SIST yields a more accurate retrieval of Z, placing the cloud between 13 and 14 km. At 18.40 UTC, the clouds are categorized as ML. The VISST retrieval is basically the same as the low cloud (blue), while the high cloud retrieval is between 9 and 14 km, certainly an improvement over the VISST retrieval. At 18.42 UTC, the ML cloudiness is misclassified as SL because the lower cloud is optically

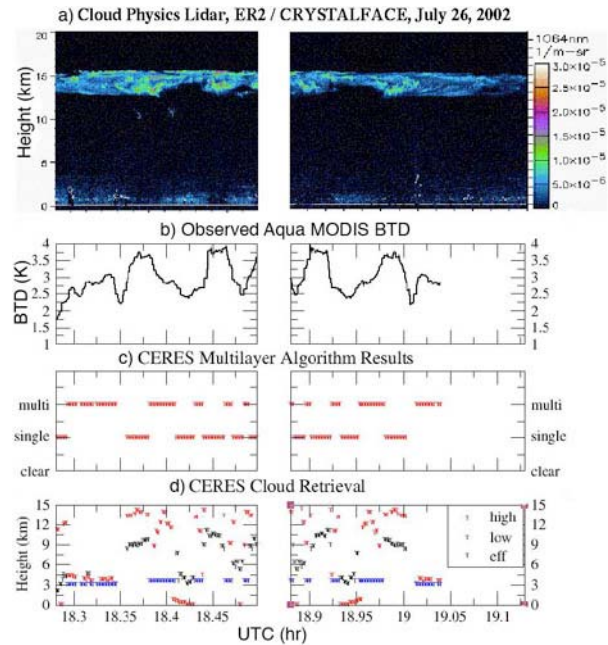


Fig. 4. Multilayered cloud case over the Gulf of Mexico with matched MODIS and ER-2 CPL data, 1830 UTC, 26 July 2002.

thin. In this case, the VISST retrieval is more accurate than the SIST. Results for the remainder of track are similar to those from the first part of the flight. This prototype retrieval is promising, but the iterations and conditions for application need to be implemented to fully assess its capabilities.

#### 4. RESULTS AND DISCUSSION

Figure 5 shows the layering classifications from the MCRS (left) and the CERES-BTD (right). The MCRS is restricted to the center of the swath because the AMSR-E scans conically at a viewing zenith angle of  $55^\circ$ . Thus, all comparisons with the MCRS use only those MODIS pixels over water taken at a viewing zenith angle of  $55^\circ$  or less. The MCRS precipitating clouds correspond to indeterminate, ML, and SL ice clouds from the CERES-BTD method as well as to some SL water clouds. The MCRS ML clouds typically correspond to different ML clouds from the CERES-BTD technique.

The comparisons with the MCRS results for all eighteen 5-minute *Aqua*-MODIS granules are quantified in Table 1. The numbers represent the percent of all MODIS pixels within the FOVs of all AMSR-E pixels over all 18 MODIS granules having an MCRS classification. Because the over all 18 MODIS granules is only used for AMSR-E pixels having at least 98% ice cloud coverage from the VISST or are precipitating, the percentages will exclude most clear and many SL and ML water pixels from consideration. The CERES-BTD yields a match of

56.3% for ML ice clouds. The CERES-BTD finds no high clouds in 31.1% of the MCRS ML cases. The CERES-BTD yields agrees with the MCRS for SL ice clouds in 54.9% of the cases. The CERES-BTD detects ML ice 38.1% of the time when MCRS detects SL ice. When the MCRS retrieves precipitating clouds (PRCP), CERES-BTD identifies roughly 10% of the PRCP as SL water clouds, 10% as SL ice clouds, and 43% as ML ice clouds.

An overall score for the CERES-BTD method relative to the MCRS retrievals can be assessed by considering only the non-precipitating AMSR-E pixels. A correct classification is assumed if the CERES-BTD technique yields ML clouds when the MCRS detects ML ice, and SL clouds when the MCRS retrieves SL water. Given that basis, the CERES-BTD yields accurate classifications in 62% of the cases. Some of the errors in the ML methods may be due to inaccuracies in matching the MODIS pixels used for the MODIS-only retrievals because the nadir FOV size was assumed for the matching. However, a comparison of the images in Fig. 1 indicate that this is not likely to explain more than a few percent of the differences in classifications. Another source of error is the assumption that, in an AMSR-E FOV, the entire area is covered by a water cloud when  $LWP > 40 \text{ gm}^{-2}$  and by no water when  $LWP < 40 \text{ gm}^{-2}$ . This is a reasonable assumption given that the detectability of  $LWP$  from MW data is highly uncertain when the  $LWP$  is below that limit and it corresponds to a lower cloud optical depth of  $\sim 5$  for  $r_e = 12 \mu\text{m}$ . Detection of ML clouds with the MODIS data alone is likely to be difficult if  $\tau < 5$ . However, if the lower clouds are scattered and have optical depths exceeding 5, then the MW-VIS-IR might classify the cloud as SL ice while the MODIS methods could classify a third or more of the pixels as ML and be correct. Conversely, the AMSR-E pixel could be half covered by optically thick cumulus clouds and be classified as ML ice while only half of the MODIS pixels are categorized as ML and be correct.

Figure 6 shows cloud layering classifications for 0220 UTC and 2200 UTC January 5, 2005. The ML clouds identified by the CERES-BTD method are color coded by the optical depth retrieved from VISST. It is seen that very few clouds are identified as ML with optical depths less than 4 (yellow and orange

colors in Figure 6). This is also true for all other 5-minute MODIS granules analyzed here (not shown). Therefore, further research on how the BTDs behave for optically thin clouds ( $\tau < 4$ ) is the next step for improving the method.

Accepting the assumption that MCRS is accurate, the BTD histograms were constructed using all MODIS pixels within the AMSR-E FOVs for the eighteen granules having an MCRS classification, with optical depth  $1 < \tau < 4$  and cloud effective temperature ranging from 200 - 270 K. Various channel combinations of BTD are  $T(11 \mu\text{m}) - T(3.7 \mu\text{m})$ ,  $T(11 \mu\text{m}) - T(4.0 \mu\text{m})$ ,  $T(11 \mu\text{m}) - T(6.7 \mu\text{m})$ ,  $T(11 \mu\text{m}) - T(12 \mu\text{m})$ ,  $T(11 \mu\text{m}) - T(8.5 \mu\text{m})$ , and  $T(11 \mu\text{m}) - T(13.3 \mu\text{m})$ . Figures 7, 8 and 9 show the relative BTD histograms for all matched MODIS pixels classified as ML or SL identified by MW-VIS-IR, for each cloud effective temperature range retrieved from VISST. T In the figures, ML clouds are represented with black and SL red. Figure 7a shows the BTD histogram for all five channel pairs and indicates that most clouds in the cloud effective temperature (retrieved by VISST) range of 200 - 210 K are SL ice cloud, although more statistics are needed to confirm the conclusion. Figures 7b, 8a, 8b, 9a, and 9b show BTDs of observed brightness temperature  $T(11\mu\text{m}) - T(8.5\mu\text{m})$ ,  $T(11 \mu\text{m}) - T(12 \mu\text{m})$ ,  $T(11 \mu\text{m}) - T(13.5 \mu\text{m})$ ,  $T(11 \mu\text{m}) - T(4.0 \mu\text{m})$ , and  $T(11 \mu\text{m}) - T(6.7 \mu\text{m})$ , respectively, for all cloud effective temperature ranges 220 - 260 K. For almost all BTDs, both SL and ML histograms have very broad curves and the majority of ML and SL curves overlap. However BTDs for  $T(11\mu\text{m}) - T(8.5\mu\text{m})$  and  $T(11\mu\text{m}) - T(4.0\mu\text{m})$  have distinct separations between ML and SL, and the BTDs of the most ML and SL pixels increase as cloud effective temperature increases. To demonstrate how the BTD study helps tuning to improve the CERES-BTD multilayer classification, a new test (BTD11-85) based on  $T(11\mu\text{m}) - T(8.5\mu\text{m})$  is added. This test uses a lookup table derived from Fig. 7b, for each cloud effective temperature bin (210 - 220K, 220 - 230K, 230 - 240K, 240 - 250K, and 250 - 260K). The look up table comprises several thresholds for each cloud effective temperature bin and is only valid for cirrus clouds with optical depth less than 4 and greater than 1, to single out multilayer clouds.

Table 1. CERES - BTD classification of MODIS pixels in marine AMSR-E pixels containing 98% ice cloud cover as determined by the VISST for the same MODIS pixels. Results in % total number of MODIS pixels, except N(AMSR).

MCRS class	SL water	SL Ice	ML water	ML ice	Indeterminate	Clear	N(AMSR)
ML ice	0.3	31.1	0.3	56.3	n/a	0.0	62197
SL ice	0.5	54.9	0.2	38.1	n/a	0.3	48119
Precipitation	10.5	10.6	2.7	43.0	n/a	1.9	102641

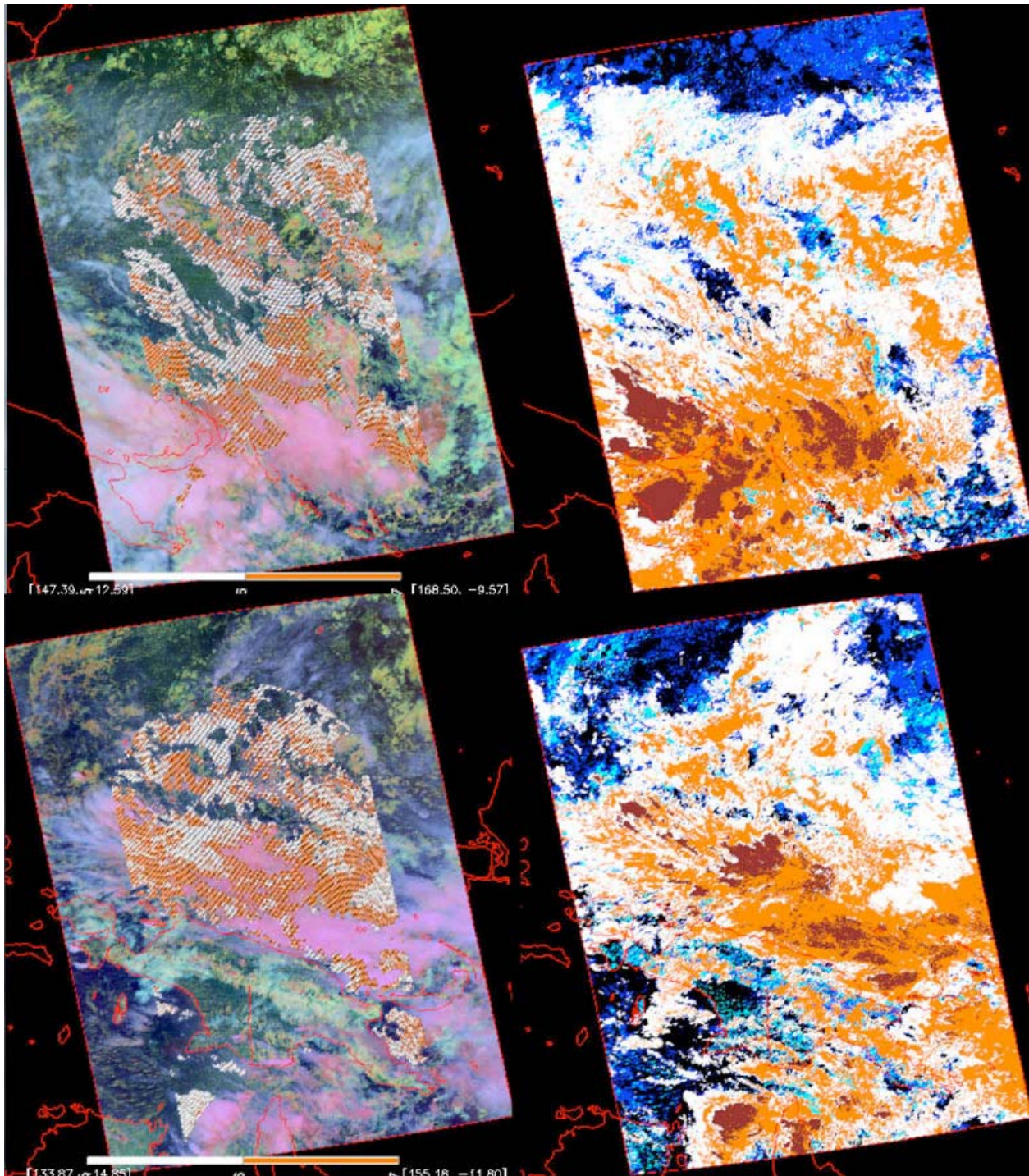


Fig. 5. Cloud layering classifications for 0400 UTC January 3, 2005 (top) and 0305 UTC January 4, 2005 (bottom). MW-VIS-IR (left): orange - ML ice, white - SL ice, else - precipitation, cloud cover < 98% in AMSR-E FOV or view angle > 55°. CERES-BTD (right): orange - ML ice, white - SL ice, dark blue - SL water, cyan - ML water, brown - thick convective clouds, black - clear.

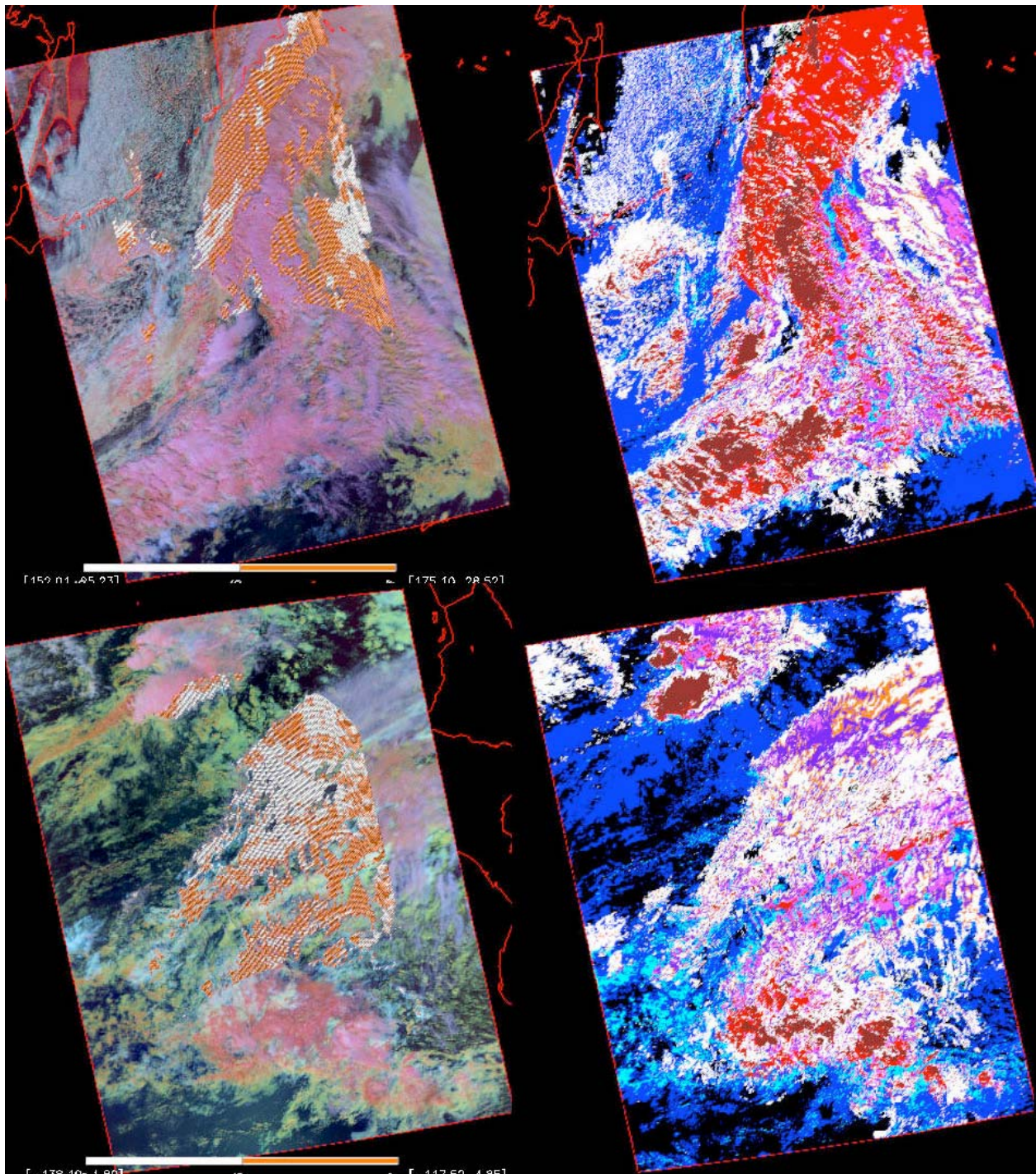


Fig. 6. Cloud layering classifications for 0220 UTC (top) and 2200 UTC January 5, 2005 (bottom). MW-VIS-IR is on the left and CERES-BTD on the right. CERES-BTD (right): yellow - ML with  $\tau < 1$ , orange - ML with  $1 < \tau < 4$ , blue purple - ML with  $4 < \tau < 8$ , magenta - ML with  $8 < \tau < 16$ , red - ML with  $16 < \tau < 128$ . The rest of colors are: white - SL ice, dark blue - SL water, cyan - ML water, brown - thick convective clouds, black - clear.

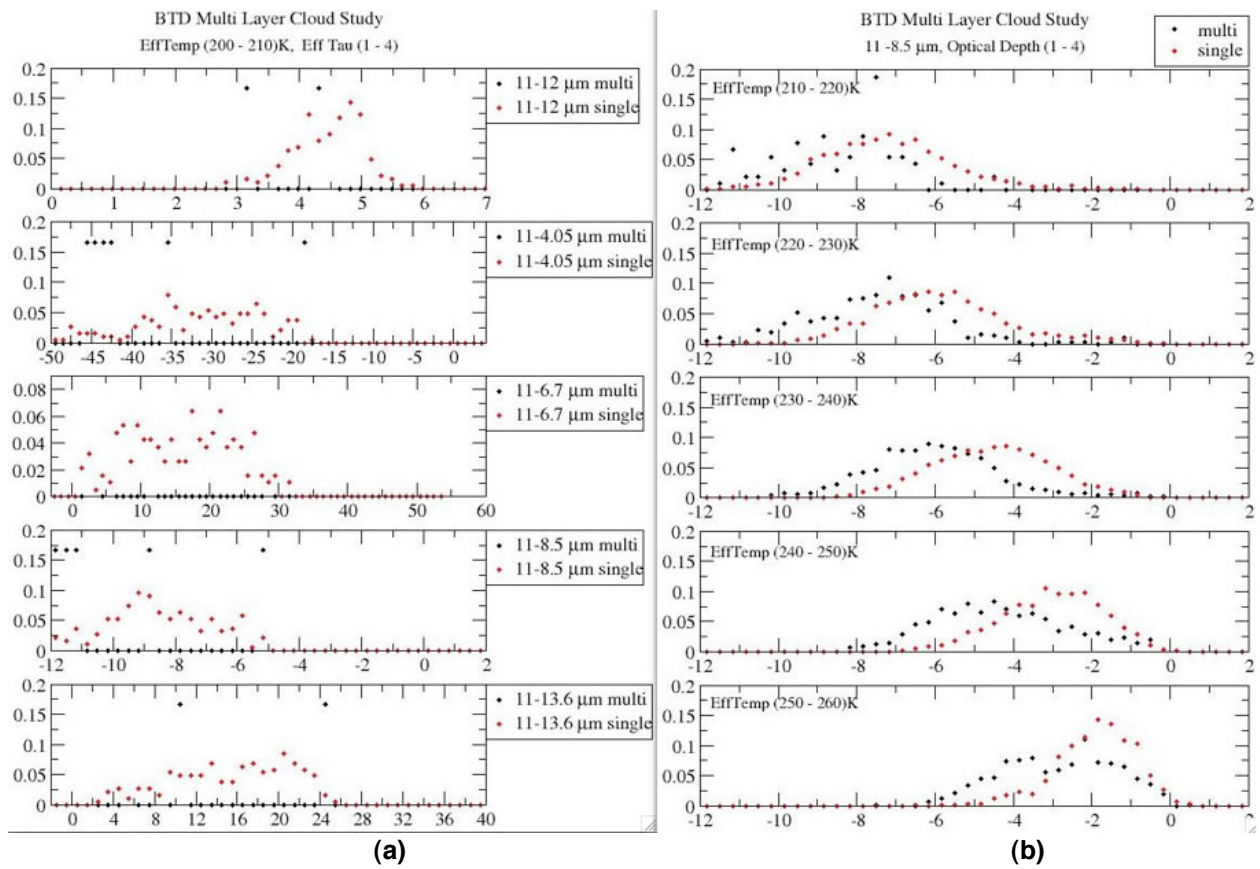


Fig. 7. Relative BTD histogram for all 18 5-minute *Aqua* MODIS granules with  $1 < \tau < 4$ . ML (black) and SL (red) are classified by MW-VIS-IR. BTD of various channel combinations (a) are for cloud effective temperature (retrieved from VISST) range of 200 - 210 K. BTD of observed brightness temperature  $T(11\mu\text{m}) - T(8.5\mu\text{m})$  (b) is sorted for each cloud effective temperature bin (10 K per bin) ranging 220 - 260 K.

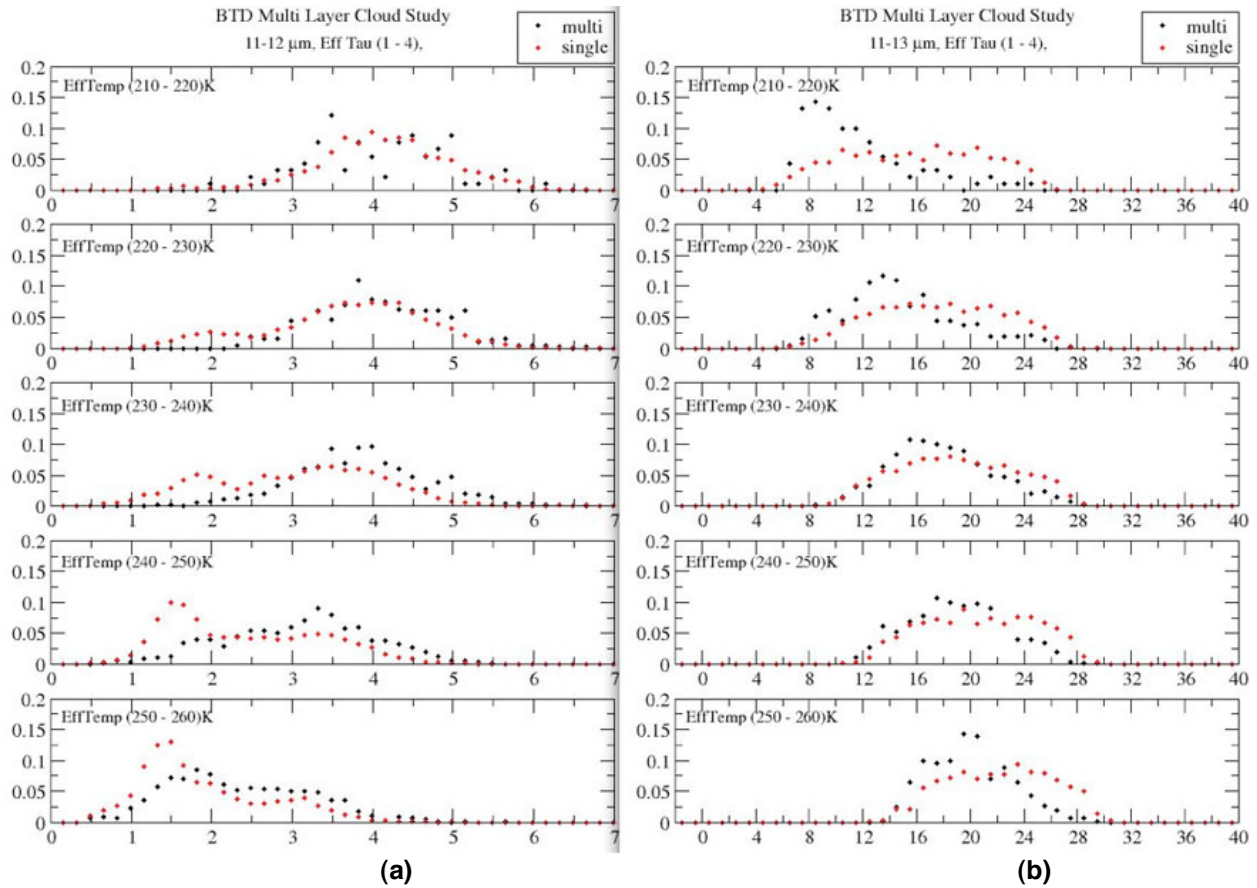


Fig. 8. Same as Fig. 7(b), except for BTDs are (a)  $T(11\mu\text{m}) - T(12\mu\text{m})$  and (b)  $T(11\mu\text{m}) - T(13.3\mu\text{m})$ .

Figure 10 shows cloud classifications from MCRS (left) overlay on the RGB image of an *Aqua* MODIS granule at 2315 UTC, 9 January 2005. Also shown are the VISST-retrieved values of  $\tau$  (Fig. 10 at right) for all cloud types assuming SL clouds. The cloud optical depths range from 1 - 4 for areas of (a) and (b) in Fig. 10 at right. The MCRS identifies mostly ML for area (a) and mostly SL for area (b) (see Fig. 10 at left). Figure 11 shows the CERES-BTD cloud layering classification without the new BTD11-85 test (left), and with BTD11-85 test (right) for the same granule as in Fig. 10. Before the implementation of the new test (BTD11-85), the CERES-BTD method classifies most SL for area (a) and lots of ML for area (b), exactly opposite of what MCRS claims. This is in a better agreement with MCRS classification. This demonstrates that by matching MODIS pixels into FOVs of AMSR-E, BTD statistics can be used to improve ML determinations. However, much more data are needed to see if the width of the broad BTD

curves (Figs. 7, 8, and 9) can be reduced, and, more importantly, to see if there really exists a clear separation between ML and SL in BTDs.

Chang and Li (2005) exploited the discrepancy between the cloud-top pressure derived from a CO<sub>2</sub>-slicing retrieval and the IR-based cloud pressure to detect overlapped clouds. This multilayer identification method (CERES-CO<sub>2</sub>-Multi) has been implemented in the CERES framework. Figure 12 shows layering classifications from all three methods, MCRS on the left, CERES-BTD in the middle and CERES-CO<sub>2</sub>-Multi on the right. The color code for CERES-CO<sub>2</sub>-Multi for ML clouds consists of yellow, orange ( $3.6 < \tau < 23$ ), red ( $\tau > 23$ ), magenta and brown (marginal ML), SL clouds with various optical depths correspond to the rest of the colors and clear pixels are shown in black. All three methods show similar ML and SL patterns, although more quantitative measurements are needed for validation.

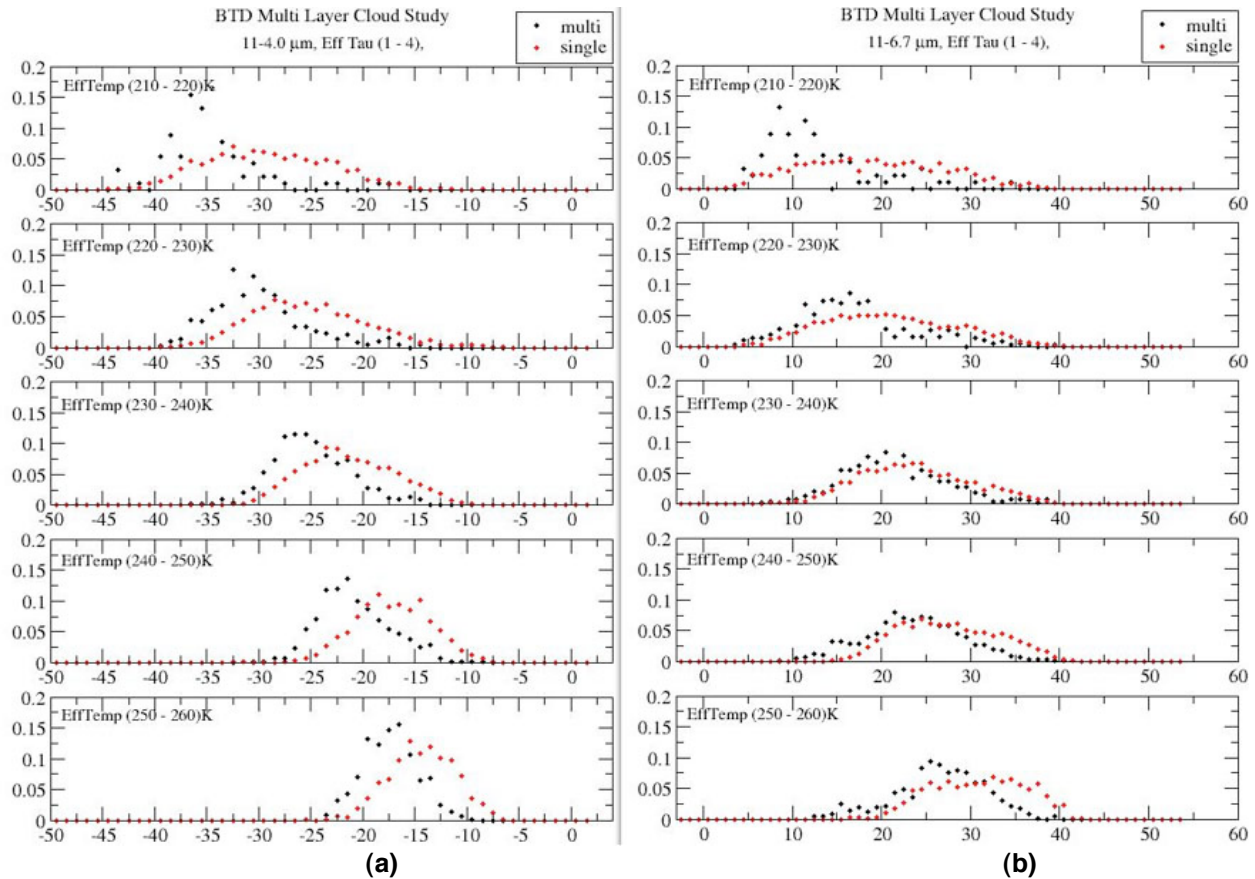


Figure 9: Same as Fig. 7(b), except for BTMs are (a) T (11 $\mu$ m) - T (4.05 $\mu$ m) and (b) T (11 $\mu$ m) - T (6.7 $\mu$ m).

## 5. CONCLUDING REMARKS

There appear to be distinct, but overlapping BTM distributions for ML and SL clouds when matching MODIS pixels to AMSR-E FOVs. The broad histograms for both ML and SL cause difficulties in creating an accurate lookup table. This confirms that passive remote sensing of multilayered cloud systems is a difficult and possibly intractable approach for a number of cloud systems. However, because only 18 scenes were analyzed, the various techniques have not been optimized, and the uncertainties and limitations of the reference MCRS method have not been clearly defined. Considerably more data need to be processed to create more accurate BTM distributions for both ML and SL clouds, and hopefully produce well-separated ML BTMs and SL BTMs. A framework for performing more detailed and robust comparisons has been established, thus, facilitating

the analysis of multilayered clouds over the global oceans and for incorporating the optimized algorithms for both published and unpublished detection methods. By further detailed examination of the MCRS in conjunction with surface, airborne, and satellite lidar-radar systems, it should be possible to determine the uncertainties in a given retrieval. The capabilities of the other methods can then be assessed using both the active sensors and the MCRS to cover more cloud types and viewing angles than would be possible using the active sensors alone.

### Acknowledgments

This research is supported by the NASA Science Mission through the CERES and CRYSTAL-FACE programs. The ER-2 image was obtained from the CPL home page, <http://cpl.gsfc.nasa.gov/>.

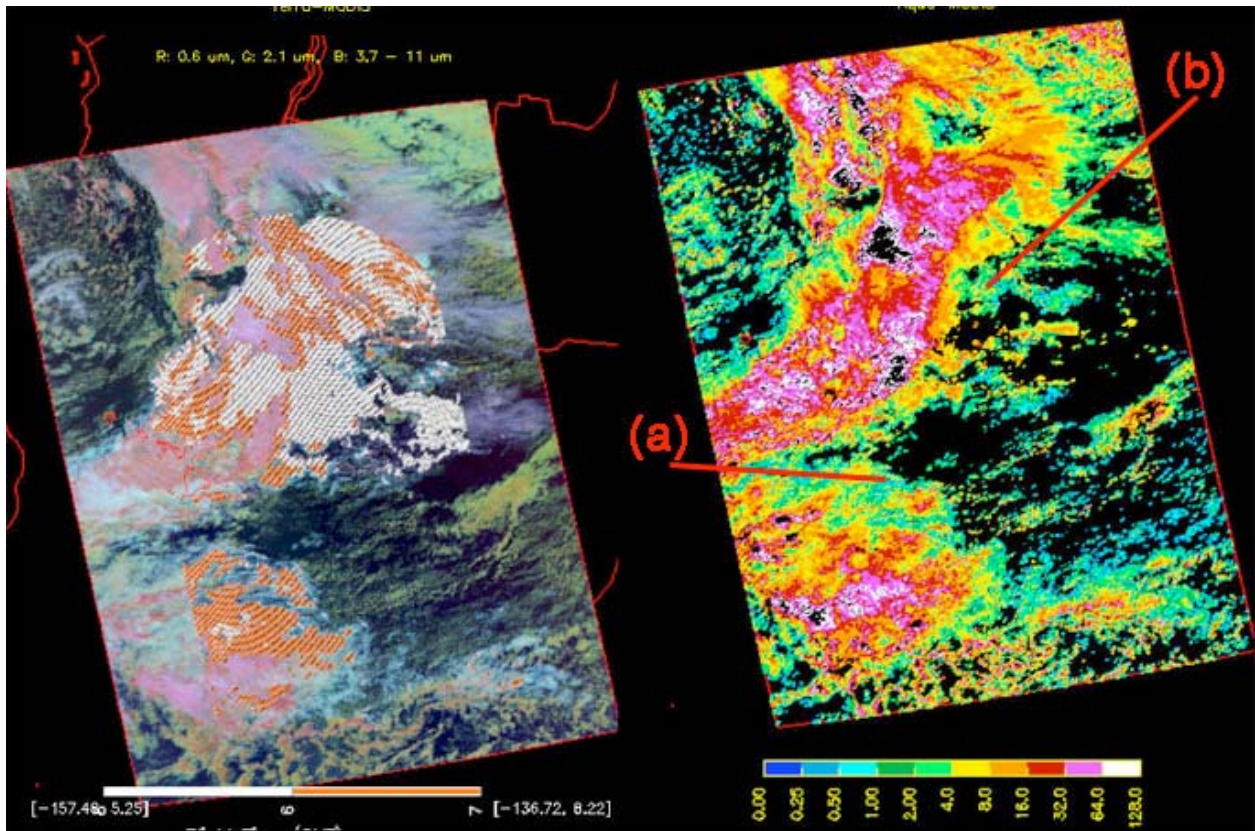


Fig. 10. CERES imagery for multilayer cloud detection comparisons for 2315 UTC, January 9, 2005. Left: Aqua MODIS pseudo-color RGB image overlaid with MW-VIS-IR cloud layering classifications: orange - ML ice, white - SL ice. Right: VISST-derived cloud optical depth, where  $1 < \tau < 4$  for areas (a) and (b).

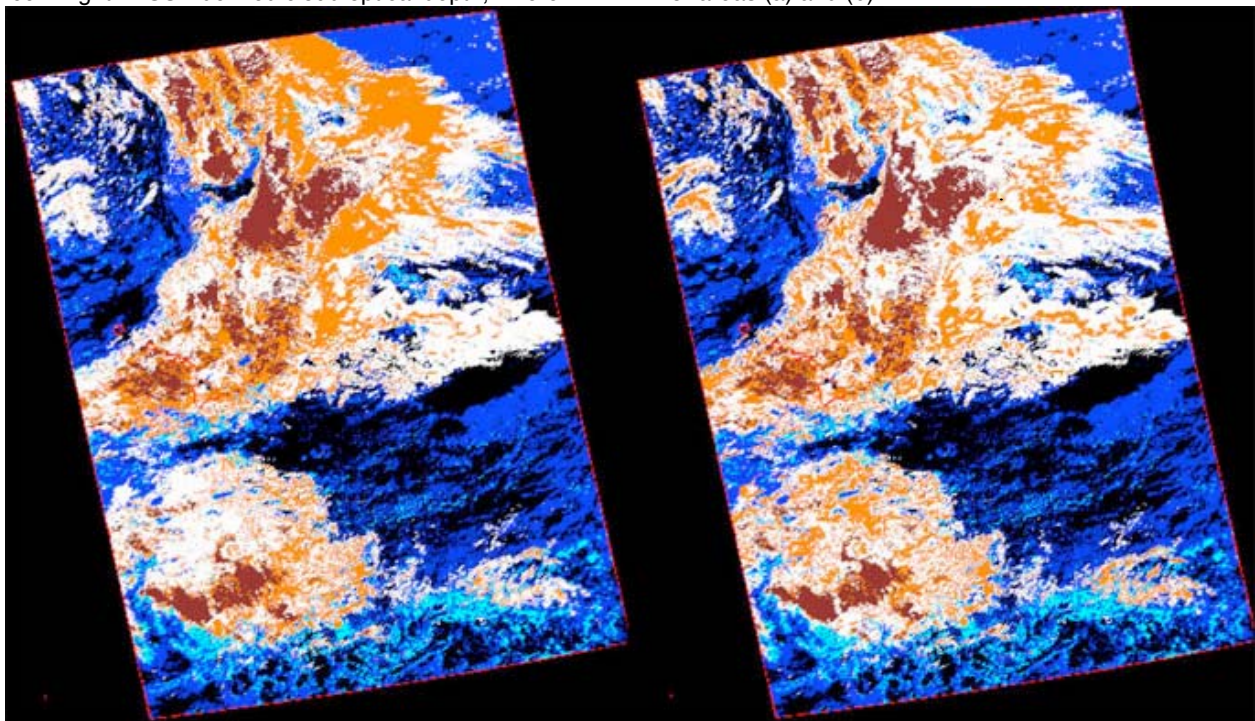


Fig. 11. CERES-BTD cloud layering classification without BTD ( $T(11 \mu\text{m}) - T(8.5 \mu\text{m})$ ) test (left), with the test (right) for 2315 UTC, January 9, 2005. The

color code is the same as Figure 5 (right).

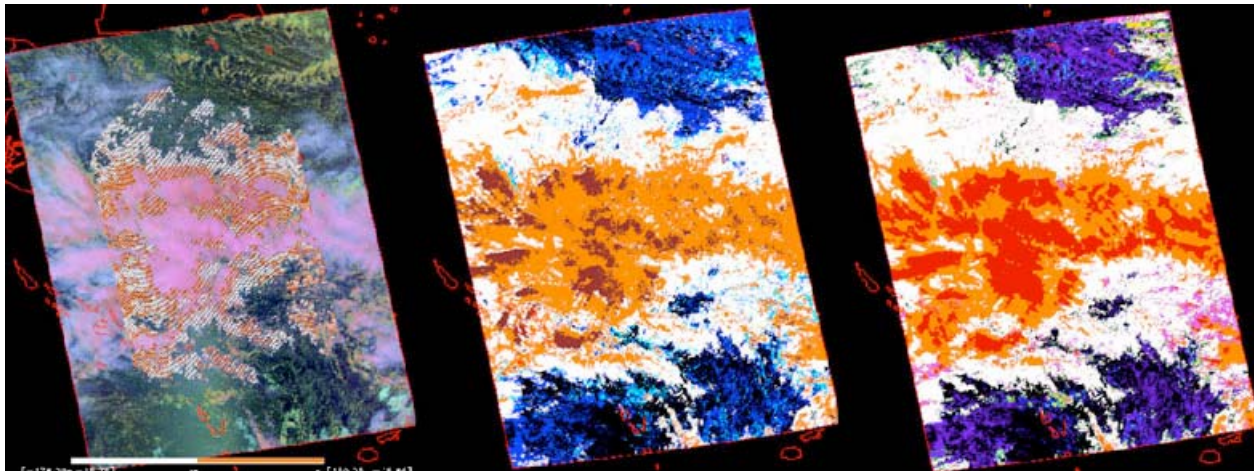


Fig. 12. Layering classifications from all three methods: MW-VIS-IR on the left, CERES-BTD in the middle and CERES-CO2-Multi on the right. The color code for CERES-CO2-Multi (right) is ML being yellow, orange ( $3.6 < \tau < 23$ ), red ( $\tau > 23$ ), magenta and brown (marginal ML), SL: rest of colors with various optical depths and clear: black.

### References

- Chang, F.-L. and Z. Li, 2005: A new method for detection of cirrus overlapping water clouds and determination of their optical properties. *J. Atmos. Sci.*, **62**, 3993-4009
- Heidinger, A. K. and M. J. Pavlonis, 2005: Global daytime distribution of overlapping cirrus cloud from NOAA's Advanced Very High Resolution Radiometer. *J. Climate*, **18**, 4772-4784.
- Lin, B., B. A. Wielicki, P. Minnis, and W. B. Rossow, 1998: Estimation of water cloud properties from satellite microwave and optical measurements in oceanic environments. I: Microwave brightness temperature simulations. *J. Geophys. Res.*, **103**, 3873-3886.
- Ho, S.-P., B. Lin, P. Minnis, and T.-F. Fan, 2003: Estimation of cloud vertical structure and water amount over tropical oceans using VIRS and TMI data. *J. Geophys. Res.*, **108**, 10.1029/2002JD003298.
- Huang, J., P. Minnis, B. Lin, Y. Yi, M. M. Khaiyer, R. F. Arduini, and G. G. Mace, 2005: Advanced retrievals of multilayered cloud properties using multi-sensor and multi-spectral measurements. *J. Geophys. Res.*, **110**, 10.1029/2004JD005101.
- Kawamoto, K., P. Minnis, and W. L. Smith, Jr., 2001: Cloud overlapping detection algorithm using solar and IR wavelengths with GOES data over ARM/SGP site. *Proc. 11th ARM Science Team Meeting*, March 18-22, Atlanta, GA, 2001. Available at [http://www.arm.gov/docs/documents/technical/conf\\_0103/author.html](http://www.arm.gov/docs/documents/technical/conf_0103/author.html).
- Lin, B., P. Minnis, B. A. Wielicki, D. R. Doelling, R. Palikonda, D. F. Young, and T. Uttal, 1998: Estimation of water cloud properties from satellite microwave and optical measurements in oceanic environments. II: Results. *J. Geophys. Res.*, **103**, 3887-3905.
- Minnis, P., D. F. Young, B. A. Wielicki, S. Sun-Mack, Q. Z. Trepte, Y. Chen, P. W. Heck, and X. Dong, 2002: A global cloud database from VIRS and MODIS for CERES. *Proc. SPIE 3<sup>rd</sup> Intl. Asia-Pacific Environ. Remote Sensing Symp. 2002: Remote Sens. of Atmosphere, Ocean, Environment, and Space*, Hangzhou, China, October 23-27, Vol. 4891, 115-126.
- Minnis, P., S. Sun-Mack, Y. Chen, H. Yi, J. L. Nguyen, M. Khaiyer, 2005: Detection and Retrieval of Multi-layered Cloud Properties Using Satellite Data *Proc. SPIE Europe International Symposium on Remote Sensing, Remote Sensing of Clouds and the Atmosphere X, Bruges, Belgium*.
- McGill, M. J., L. Li, W. D. Hart, G. M. Heymsfield, D. L. Hlavka, P. E. Racette, L. Tian, M. A. Vaughan, and D. M. Winker, 2004: Combined lidar-radar remote sensing: Initial results from CRYSTAL-FACE. *J. Geophys. Res.*, **109**, doi: 10.1029/2003JD004030, 2004.
- Pavlonis, M. J. and A. K. Heidinger, 2004: Daytime cloud overlap detection from AVHRR and VIIRS. *J. Appl. Meteorol.*, **43**, 762-778.